Anurans from the Early Miocene of Chamtwara (western Kenya), and the first fossil record for Arthroleptidae (Afrobatrachia, Ranoidea)

Alfred Lemierre, Martin Pickford, Brigitte Senut, Dominique Gommery

Anurans from the Early Miocene of Chamtwara (western Kenya), and the first fossil record for Arthroleptidae (Afrobatrachia, Ranoidea)

Alfred Lemierre[1] · Martin Pickford[2] · Brigitte Senut[2] · Dominique Gommery[3]

1. Royal Tyrrell Museum of Palaeontology, Box 7500 Drumheller, Alberta, Canada T0J 0Y0 alfred.lemierre@gov.ab.ca
2. Centre de Recherche en Paléontologie – Paris (CR2P, UMR 7207), MNHN/CNRS/SU, Muséum nationale d'Histoire naturelle, 8 rue Buffon, 75005 Paris, France brigitte.senut@mnhn.fr, martin.pickford@mnhn.fr
3. Centre de Recherche en Paléontologie – Paris (CR2P, UMR 7207), MNHM/CNRS/SU, Sorbonne Université, Campus Pierre et Marie Curie, T.46-56, E.5, case 104, 4 Place Jussieu, 75252 Paris cedex, France dominique.gommery@sorbonne-universite.fr

Abstract

Even though anurans are present throughout eastern Africa today, their fossil record is limited to a few localities in the Oligocene and Pliocene. Here we increase knowledge about the fossil record of East African anurans by reporting on seven isolated bones from the Lower Miocene locality of Chamtwara, Kenya. Although thousands of fossils have been collected from this locality, only mammals and gastropods have been described. The frog bones are identified as belonging to an indeterminate species of *Leptopelis* (humerus), an indeterminate neobatrachian (humerus) and one or more indeterminate anurans (femur and tibiofibulae). The humerus assigned to *Leptopelis* sp. is compared to humeri from all Sub-Saharan arthroleptid and hyperoliid genera, providing the first overview of the humeral diversity of these two large afrobatrachian families. The Chamtwara *Leptopelis* species marks the first fossil occurrence of the Arthroleptidae and the oldest occurrence of an afrobatrachian, the fossil record of which was previously limited to the Plio-Pleistocene. This species of *Leptopelis* is likely closely related to Western and Central African species of *Leptopelis* rather than to species found in East Africa today, suggesting that by the Early Miocene the latter had already diverged from the former. This pushes the divergence between those geographical groups from the Middle Miocene (~ 10 Ma) back to at least the Early Miocene (~20 Ma).

Keywords Anura · East Africa · Early Miocene ·Kenya ·Afrobatrachia

Introduction

Anurans are highly diverse in Africa today, with more than a thousand species known across the continent (Channing & Rödel 2019). However, their fossil record currently does not match this diversity, with most African families lacking a fossil record older than the Pliocene (Gardner & Rage 2016; Blackburn et al. 2019; Matthews et al. 2023; Lemierre et al. 2024). The scarcity of fossils from the Palaeogene and Miocene of Sub-Saharan Africa hampers our understanding of the diversification and evolution of most frogs in that region over the last 50 million years. During the Eocene–Oligocene, most of Sub-Saharan Africa experienced a hot and humid climate, and extensive forested environments were established across the region (Jacobs et al 2010). However, during the Miocene, uplift of the East African dome (Pickford 1990) and development of the East African Rift (Partridge 2010) profoundly impacted the climate and environment of the continent. This led to an aridification across much of Sub-Saharan Africa, with the consequence that forested environments shrank and were restricted to the highlands and other high-altitude areas (Feakins & Demenocal 2010; Jacobs et al 2010; Reichgelt & West 2025). Anuran families were profoundly impacted, as populations became progressively isolated. Distinct geographical groups within Sub-Saharan Africa have been recognized for anuran families (Neĉas et al. 2021; Portik et al. 2023) and molecular clock analyses estimate divergences among groups occurred during the Miocene (Idris 2004; Reyes-Velasco et al. 2018; Neĉas et al. 2021). As such, the poor Palaeogene and Miocene fossil record hinders our comprehension of the diversity of African frogs before and during the development of the East African dome and East African Rift and renders it difficult to document palaeobiogeographical patterns of divergence and diversification of frogs during the Neogene in Sub-Saharan Africa.

In East Africa, even though hundreds of Neogene localities, dating from the Early Miocene to the Late Pleistocene (Pickford 1983, 1986), have been studied in the past decades, few have yielded anuran remains (Gardner & Rage 2016; Delfino 2020). In particular, we have no information about anurans from Miocene localities in East Africa, even though anurans from that region have been described from the Oligocene (Ptychadenidae and Pipidae: Blackburn et al. 2015, 2019) and the Pliocene (Hemisotidae: Delfino 2020). That large temporal gap within the anuran fossil record in East Africa might be explained by palaeoenvironmental or taphonomic factors that were not favorable for the preservation of anuran remains (Dodson 1973; Tappen 1994).

Most of the Miocene vertebrate localities in East Africa are in Kenya, where fossils have been collected over several decades (Pickford 1986). Palaeoenvironmental reconstructions have proposed that the western part of the country was covered by a tropical forest, an environment today restricted to the Shimba Hills (southwestern Kenya) and Kakamega Forest (western Kenya). Seven anuran postcranial elements have been identified within the rich Lower Miocene hominoid locality of Chamtwara, southwestern Kenya (Fig. 1). The presence of anurans within a humid tropical forest during the Miocene in Kenya could provide information regarding anuran diversification in the region, as similar environments in East Africa are today restricted just to a few areas (Mabira, eastern Uganda; Kakamega and Shimba Hills, Kenya; Eastern Arc of Tanzania; Highlands of Ethiopia; Imatongs, South Sudan; Reichgelt & West 2025).

Here we describe and identify anuran fossils from Chamtwara and evaluate the potential insights that they provide into the early Neogene diversity and evolution of East African anurans.

Geological context

Chamtwara is located in southwestern Kenya (Fig.1). This locality is part of a large assemblage of Mio-Pliocene sites in the Nyanza Rift valley discovered since the 1970s and known for its rich diversity of mammals, including several species of hominoids (Pickford 1986; Pickford & Kunimatsu 2005; Begun 2015). The environment around the locality today is a forested savannah (Reichgelt & West 2025).

The fossiliferous layers at Chamtwara consist of red palaeosols underlain by calcified tuffs and overlain by grey tuffs (Pickford 1981). The underlying and overlying tuffs yielded a radiochronological age estimate between 20–18.5 Ma, placing this locality within the Early Miocene (Burdigalian: Pickford 1983, 2007). Since its discovery in the 1970s, Chamtwara has yielded a rich and diverse vertebrate fauna, with more than 70 taxa identified (Pickford 1986, 2007). Among them, a few squamate families were mentioned, but no specimens have been described (Pickford 1986). In addition, several gastropod species have also been identified and used to reconstruct the palaeoenvironment, as being a humid tropical forest (Pickford 1986).

Materials and methods

Specimens examined and terminology

All frog fossils reported herein were discovered in 2005 by the Kenya Palaeontology Expedition part of the project Paléontologie de l'Afrique Sub-Saharienne and are curated at the Orrorin Community Organisation, Baringo County in Kenya.

We compared our fossil humeri to 85 specimens from 83 species, 52 genera and 13 neobatrachian families found in Sub-Saharan Africa using available CT-scan and 3D models on Morphosource (Blackburn et al. 2024; Table S1). We excluded four genera (*Anhydrophryne*, *Microbatrachella*, *Natalobatrachus* and *Poyntonia*) assigned to Cacosterninae (Pyxicephalidae) because they are restricted to small, isolated areas in southern Africa (Channing & Rödel 2019).

We focused our efforts on two families of afrobatrachians, Hyperoliidae and Arthroleptidae, because their osteology is poorly documented. Using available CT-data, we included 22 species (out of 224) from 12 hyperoliid genera (out of 17) and 19 species (out of 151) from all eight arthroleptid genera (Table S2). We also added comparisons to the Brevicipitidae and Hemisotidae using the literature (Van Dijk 2006 for Brevicipitidae; Delfino 2020 for Hemisotidae).

CT-scan data were all imported into the 3D reconstruction software 3D Slicer (https://www.slicer.org/; Fedorov et al. 2012). Before importing, slices were cropped to remove empty space, and contrast was adjusted for better reconstruction. 3D models were produced by segmenting of each bone using the 'thresholding' function (using the contrast on greyscale images). In total, 75 3D models of right humeri were produced and exported as separate stl files (Tables S1, S2). They were subsequently exported on MorphoSource (see Tables S1, S2). Ten specimens were not segmented, because 3D models of their right humeri are already available on MorphoSource (see Tables S1, S2).

The anatomical nomenclature used herein follows Bolkay (1919) and Sanchíz (1998). Anuran taxonomy follows Portik et al. (2023) and Frost (2024).

Institutional abbreviations

CAS: HERP: California Academy of Sciences Herpetology collection, San Francisco, California, USA;

OCO-KOR: Orrorin Community Organisation, Koru collection, Kipsaraman Museum, Tugen Hills, Kenyal;

UF-HERP: University of Florida Herpetology collection, Gainesville, Florida, USA;

ZMB: Museum für Naturkunde, Berlin, Germany.

Systematic palaeontology

Anura Duméril, 1805

Neobatrachia Reig, 1958

Ranoidea Frost, Grant, Faivovich, Bain, Haas, Haddad, De Sá, Channing, Wilkinson, Donnellan, Raxworthy, Campbell, Blotto, Moler, Drewes, Nussbaum, Lynch, Green, & Wheeler, 2006

Afrobatrachia Frost, Grant, Faivovich, Bain, Haas, Haddad, De Sá, Channing, Wilkinson, Donnellan, Raxworthy, Campbell, Blotto, Moler, Drewes, Nussbaum, Lynch, Green, & Wheeler, 2006

Arthroleptidae Mivart, 1869

Leptopelinae Laurent, 1972

Leptopelis Günther, 1859

Leptopelis sp.

(Figs. 2a–d, 3a–d, 4a–d, 5a–d, 6a–d, 7a–d, 8a–d, 9a–d, 10a–d)

Referred specimen: OCO-KOR 502'05d, almost complete right humerus.

Osteological description: The humerus (Fig. 2a–d) is almost complete, apart from the caput humeri. The diaphysis is slender and gently curved ventrally (Fig. 2a, d). In dorsal and ventral views, the proximal region is slightly curved laterally (Fig. 2a, d). On the ventral surface of the humerus, the crista ventralis extends proximally from the caput humeri to the level of the mid-diaphysis (Fig. 2a). The crista ventralis is well developed proximally (i.e., as wide as the diaphysis: Fig. 2a). The fossa cubitalis ventralis is shallow, not well defined and extends transversely along the proximal margin of the eminentia capitata (Fig. 2a). The eminentia capitata is incompletely preserved (Fig. 2a). Both epicondyles are broken off distally (Fig. 2a–c). The epicondylus ulnaris is more prominently developed than the epicondylus radialis (Fig. 2a), with the latter likely poorly distinct from the eminentia capitata (Fig. 2a). A small crista lateralis is present along the distal portion of the lateral margin of the humerus (Fig. 2b). A faint crista medialis is present along the distal portion of the medial margin, mostly visible in medial view (Fig. 2c). In the proximal region, a thin and well-marked crista paraventralis is present medially (Fig. 2c). On the dorsal surface, the olecranon scar is small and tapers proximally (Fig. 2d).

Attribution: Sub-Saharan Africa is inhabited, both in the fossil record and currently, by two main clades, Pipidae and Neobatrachia (Gardner & Rage 2016; Channing & Rödel 2019). The presence of asymmetrical epicondyles and a curved diaphysis excludes an assignment to Pipidae (Gómez 2016). Among Neobatrachia, 15 families are recognized in Sub-Saharan Africa: Heleophrynidae; one (Bufonidae) assigned to Hyloidea; and 13 assigned to the large Ranoidea (Portik et al. 2023).

OCO-KOR 502'05d differs from *Hadromophryne* (Fig. 3e–h), one of two genera recognised within Heleophrynidae, in having (1) a wider diaphysis, (2) a more developed epicondylus radialis (indistinct from the eminentia capitata in *Hadromophryne*), (3) a crista ventralis more extended distally, and (4) its diaphysis arched ventrally in lateral or medial views.

We compared OCO-KOR 502'05d to 11 genera (out of the 13 identified in Sub-Saharan Africa; Channing & Rödel 2019) from the cosmopolitan family Bufonidae (Hyloidea). Our fossil specimen can be excluded from *Mertensophryne* (Figs. 3i–l, S1), *Poyntonophrynus* (Fig. S1) and *Sclerophrys* (Figs. 3m–p, S1) in having its eminentia capitata on the diaphyseal axis (in the three bufonid genera, the eminentia capitata has shifted from the diaphyseal axis). It can be differentiated from *Nectophrynoides* (Figs. 3q–t, S1) in having (1) its proximal region curved laterally (straight in *Nectophrynoides*) and (2) its diaphysis arched ventrally (vs. almost straight diaphysis in *Nectophrynoides*). OCO-KOR 502'05d differs from *Schismaderma carens* (Figs. 3u–x, S1), *Capiensibufo* (Fig. S2), *Didynamipus* (Fig. S2), *Nectophryne* (Fig. S2), *Vandijkophrynus* (Fig. S2) and *Werneria* (Fig. S2) in having its diaphysis curved laterally in dorsal or ventral views (straight in all four bufonid genera). OCO-KOR 502'05 can be additionally differentiated from *Capiensibufo*, *Didynamipus* and *Nectophryne* in having its eminentia capitata on the diaphyseal axis. OCO-KOR 502'05 differs from *Wolterstorffina* (Fig.

S2) in (1) lacking the expanded cristae lateralis and medialis, (2) lacking a thick crista ventralis, (3) having its diaphysis curved laterally in dorsal or ventral views and (4) having its eminentia capitata on the diaphyseal axis.

Three major clades are recognised for Ranoidea (Hime et al. 2021; Portik et al 2023): Natatanura; Microhylidae; and Afrobatrachia. Natatanura contains most African anuran families (nine families: Feng et al 2017). OCO-KOR 502'05d is excluded from *Chiromantis* (Figs. 4e–h, S3), the sole genus of African Rhacophoridae, in having a thicker diaphysis curved laterally in dorsal or ventral views. It is excluded from Conrauidae (monogeneric family) in having an olecranon scar located on the lateral portion of the dorsal surface of the humerus (central in *Conraua*: Figs. 4i–l, S3). OCO-KOR 502'05d differs from *Hoplopbatrachus occipitalis* (Figs. 4m–p, S3), the sole African species of Discroglossidae, in having its diaphysis curved laterally in dorsal or ventral view and in bearing a more developed crista ventralis. Within Petropedetidae (two genera recognised), OCO-KOR 502'05d is excluded from *Arthrolepides* (Fig. S3) and *Petropedetes* (Figs. 4q–t, S3) in having a thicker diaphysis with a higher crista ventralis and lacks a developed cristae lateralis and medialis. OCO-KOR 502'05d differs from both *Odontobatrachus* (Figs. 4u–x, S3), the sole genus of Odontobatrachidae, and *Phrynobatrachus* (Figs. 4y–bb, S3), the sole genus of Phrynobatrachidae, in having a thicker diaphysis bearing a higher crista ventralis. OCO-KOR 502'05d further differs from *Phrynobatrachus* (Figs. 4y–bb, S3) in having a more developed epicondylus radialis. OCO-KOR 502'05d is excluded from *Ptychadena* (Figs. 5e–h, S4) and *Hildebrantia* (Fig. S3), two of the three genera of Ptychadenidae, in having a diaphysis curved laterally in dorsal or ventral views. OCO-KOR 502'05d differs from *Amnirana* (Figs. 5i–l, S4), the sole African genus of Ranidae, in having (1) the diaphysis curved laterally in ventral view (straight in *Amnirana*), (2) a more developed

epicondylus radialis (indistinct from the eminentia capitata in *Amnirana*), and (3) a more developed crista ventralis.

The last natatanuran family is Pyxicephalidae, comprised of the subfamilies Pyxicephalinae and Cacosterninae. OCO-KOR 502'05d is excluded from the two genera of Pyxicephalinae, *Aubria* (not figured) and *Pyxicephalus* (Figs. 5m–p, S5), in having (1) an olecranon scar located on the lateral portion of the dorsal surface of the humerus and (2) a diaphysis more curved laterally in dorsal or ventral views. OCO-KOR 502'05d differs from four (out of 10) cacosternine genera, *Amietia* (Fig. S5), *Arthroleptella* (Fig. S5), *Cacosternum* (Figs. 5q–t, S5) and *Strongylopus* (Figs. 5u–x, S5) in having its diaphysis curved laterally in dorsal or ventral views, a crista lateralis (absent in all four genera) and a high crista ventralis extending distally up to the mid point of the diaphysis. It differs from another cacosternine genus, *Tomopterna* (Figs. 5y–bb, S5) in having a thicker diaphysis bearing both cristae lateralis and medialis, OCO-KOR 502'05d differs from the cacosternine *Nothophryne* (Fig. S5) in having its eminentia capitata on the diaphyseal axis.

Two subfamilies and three genera of Microhylidae are present in Africa (including Kenya; Spawls et al. 2019), Hoplophryninae (*Hoplophryne* and *Parahoplophryne*) and Phrynomantinae (*Phrynomantis*). OCO-KOR 502'05d differs from the humerus of *Hoplophryne* (Figs. 6e–h, S6) in (1) having a larger crista ventralis and (2) possessing a more developed epicondylus ulnaris. OCO-KOR 502'05d differs from *Phrynomantis* (Fig. 6i–l) in (1) having a larger fossa cubitalis ventralis and (2) lacking a ventral crest shifted laterally from the diaphyseal axis.

The last ranoid clade, Afrobatrachia, contains four families (Portik et al. 2023): Brevicipitidae; Hemisotidae (both not figured here); Hyperoliidae; and Arthroleptidae. OCO-

KOR 502’05d is excluded from both Brevicipitidae and Hemisotidae, because their humeri are far more robust than our specimen (Van Dijk 2000; Delfino 2020). Hyperoliidae, comprised of two recognised subfamilies, Hyperoliinae and Acanthixalinae, are one of the most diverse African families, with more than 250 species recognised, a majority of which belong to the subfamily Hyperoliinae and genera *Hyperolius* and *Afrixalus* (Channing & Rödel 2019; Frost 2024). OCO-KOR 502’05d differs from humeri of all studied hyperoliines (Figs. 7e–l; S7, S8) in being twice their size and having a thicker diaphysis bearing a more developed crista ventralis (extending up to the midpoint of the diaphysis vs. limited to distal one-third in Hyperoliinae). OCO-KOR 502’05d further differs from the hyperoliines *Kassinula* (Fig. S8) and *Opisthothylax* (Figs. 7i–l, S8) in having a more developed epicondylus radialis. OCO-KOR 502’05d differs from the monospecific Acanthixalinae (not figured) in having a more developed crista ventralis and a more reduced fossa cubitalis ventralis. We exclude OCO-KOR 502’05d from two genera of Western African hyperoliids not assigned to any subfamily, *Callixalus* (Fig. S8) and *Chrysobatrachus* (Figs. 7m–, S8p) in having a more developed epicondylus radialis (vs. epicondylus radialis pressed against the eminentia capitata in *Callixalus* and *Chrysobatrachus*). OCO-KOR 502’05d also differs from the four genera of Kassinae, *Hylambates* (Figs. 7q–t, S8), *Kassina* (Figs. 7u–x, S8), *Paracassina* (Figs. 7y–bb, S8) and *Semnodactylus* (Fig. S8), in having a thicker diaphysis with a more developed crista ventralis.

The last afrobatrachian family is Arthrolpetidae (151 species: Channing & Rodel 2019; Frost 2024). Within this family, three subfamililes are recognised: Arthroleptinae; Astylosterninae; and Leptopelinae (Hime et al. 2021). OCO-KOR 502’05d differs from the two arthroleptine genera, *Arthroleptis* (Figs. 8e–h, S9) and *Cardioglossa* (Figs. 8i–l, S8), in having a more developed epicondylus radialis and bearing a crista ventralis extending along the distal half

of the diaphyseal length vs. limited to the distal one-third of diaphyseal length in most species of *Arthrolepis*. It differs further from most arthroleptines species in having a wider and curved diaphysis (slender and straight diaphysis in most arthroleptines).

In Astylosterninae, five genera are currently recognised (Channing & Rödel 2019). OCO-KOR 502'05d differs from *Astylosternus* (Figs. 8m–p, S10), *Nyctibates* (Figs. 8q–t, S10), *Scotobleps* (Figs. 8u–x, S10) and *Trichobatrachus* (Figs. 8y–bb, S10) in having a laterally curved diaphysis in dorsal and ventral views. It further differs from *Astylosternus* (Fig. 8m–p), in having a more elongate crista ventralis. The last astylosternine genus, *Leptodactylodon* (Figs. 8cc–ff, S10), differs from OCO-KOR 502'05d in having a less developed epicondylus radialis and a more slender diaphysis.

Leptopelinae is composed of a single genus, *Leptopelis* (54 recognised species: Frost 2024). Compared to the six species of *Leptopelis* available to us for comparisons, OCO-KOR 502'05d most closely resembles two species, *Leptopelis bocagii* (Fig. 9e–h) and *L. nordequatorialis* (Fig. 9i–l), and differs from the other four species (Fig. 9m–bb), in having (1) a diaphysis curved laterally in dorsal and ventral views, (2) a crista ventralis extending distally up to the midpoint of the mid-diaphysis, (3) a well-marked and thin crista paraventralis, (4) a shallow and not well-delimited fossa cubitalis ventralis and (5) an epicondylus slightly projecting from the eminentia capitata.

We assign OCO-KOR 502'05d to Leptopelinae because (1) the above-listed osteological features differentiate it from humeri of other genera in subfamilies and families of Sub-Saharan neobatrachians and (2) of osteological similarities with humeri of *Lepotpelis bocagii* and *L. nordequatorialis* listed above. Because Leptopeline is only composed of *Leptopelis*, we assign our specimen to this genus. Interestingly, OCO-KOR 502'05d is most similar to the humerus

from a juvenile of *L. bocagii* (Fig. 10e–h), rather than to an adult female (Fig. 10i–l) or male (Fig. 10m–p) of that species. Thus, it is possible that OCO-KOR 502'05d belongs to a juvenile *Leptopelis.* Because the osteology (especially the humerus) of *Leptopelis* has never been adequately documented (Drewes 1984; Idris 2004; Scott 2005), we refrain from any assignment beyond *Leptopelis* sp., but we recognize OCO-KOR 502'05d is similar to *L. bocagii* and *L. nordequatorialis*.

Neobatrachia indet.

(Fig. 11a, b)

Referred specimen: OCO-KOR 502'05e, distal portion of a left humerus.

Osteological description: OCO-KOR 502'05e is an incomplete left humerus (Fig. 11a–b) preserving only part of the distal end. Based on its preserved distal portion, the diaphysis is slender (Fig. 11a). The fossa cubitalis ventralis is shallow and reduced, extending transversely along the proximal margin of the poorly preserved eminentia capitata (Fig. 11a). Both epicondyles are broken but appear to have been poorly developed and asymmetrical, with the epicondylus ulnaris more developed (Fig. 11a). In dorsal view, the olecranon scar is small and rounded (Fig. 11b).

Attribution: OCO-KOR 502'05e can be excluded from all known pipids based on the presence of a reduced fossa cubitalis ventralis extending along the proximal margin of the eminentia capitata and asymmetrical epicondyles (epicondyles symmetrically developed in Pipidae: Gómez 2016). OCO-KOR 502'05e, with its poorly developed epicondyles and a small, rounded olecranon scar, is similar to a humerus illustrated by Delfino (2020: fig. 3) from a Lower

Pliocene locality in northern Kenya. That Pliocene humerus has been assigned as to an indeterminate neobatrachian taxon (Delfino 2020). Because OCO-KOR 502'05e is too poorly preserved to be identified more precisely, we also identify it as belonging to an indeterminate neobatrachian taxon.

Anura indet.

(Fig. 11c, d)

Referred specimens: OCO-KOR 502'05f, proximal? portion of a femur; OCO-KOR 502'05g–j, four indeterminate portions of tibiofibulae.

Osteological description: OCO-KOR 502'05f only preserves the captut femoris (Fig. 11c). OCO-KOR 502'05g–j consist of either the proximal or distal regions of four tibiofibulae Fig. 11d).

Attribution: Because OCO-KOR 502'05f (femur) and OCO-KOR 502'05g–j (tibiofibulae) are fragmentary and neither element is especially diagnostic, none of these fossils can be attributed to any anuran clade.

Discussion

Miocene anurans in East Africa

Within East Africa, anurans previously have been recorded from three localities (Fig. 1b): the Upper Oligocene Nsungwe Formation in Tanzania (Pipidae and Neobatrachia: Ptychadenidae: Blackburn et al. 2015, 2019); the Miocene locality of Maboko Island, Kenya (Andrews et al. 1981; Gardner & Rage 2016); and the Lower Pliocene locality of Kanapoi, Kenya (Neobatrachia: Hemisotidae; Delfino 2020). Anuran fossils from Maboko Island have neither been described nor illustrated, making it impossible to compare them to the Chamtwara fossils. According to Andrews et al. (1981), Maboko Island yielded 52 anuran bones belonging to five anuran taxa. A second Lower Miocene locality, Napak XV in Uganda, has yielded a caecilian skull (Pickford 2004; Rage & Pickford 2011), but no anuran fossils (Gardner & Rage 2016). Thus, the anurans from Chamtwara help fill a temporal gap (Early Miocene) within the East African fossil record of anurans.

Although Afrobatrachia (living only in Africa, Madagascar and Seychelles) are one of the three main clades of ranoids, until now the fossil record of its four families was restricted to the Plio-Pleistocene of continental Africa (Gardner & Rage 2016; Delfino 2020). Thus, the Chamtwara *Leptopelis* marks the oldest known occurrence of Afrobatrachia in the fossil record. Furthermore, it is also the first known fossil record of an arthroleptid, because other afrobatrachian occurrences belong to the other three afrobatrachians families (Brevicipitdae, Lower Pliocene: Matthews et al. 2015; Hemisotidae, Lower Pliocene: Delfino 2020; Hyperoliidae, Lower Pliocene: Matthews et al 2015).

Leptopelis palaeobiogeography and evolutionary history

The genus *Leptopelis* (forest treefrogs, leaf frogs) is known throughout sub-Saharan Africa (Channing & Rödel 2019). This genus contains a large diversity (54 species) of morphologically different species, present in various environments and regions of the continent. As such, several "groups" are recognized within this genus, such as the Ethiopian *Leptopelis* (Reyes-Velasco et al. 2018) and Albertine Rift *Leptopelis* (Portillo et al. 2015). Furthermore, three subgenera have been proposed within *Leptopelis* ("*Elaphromantis"*, "*Heteropelis"*, and "*Taphriomantis"*: Laurent 1941). This large diversity has been linked to major environmental changes during the late Palaeogene and Neogene (Portillo et al. 2015; Portik 2015; Portik & Blackburn 2016; Reyes-Velasco et al. 2018). The earliest divergence is between the basal *Leptopelis parkeri* and all other *Leptopelis*, estimated to have taken place during the Eocene (note: *L. parkeri* is sufficiently different from all other *Leptopelis* and could be assigned to its own genus: Portik 2015; Portik & Blackburn 2016). Further divergence and diversification events within *Leptopelis* are estimated to have occurred during the Mio-Pliocene (Portillo et al 2015; Portik & Blackburn 2016; Reyes-Velasco et al. 2018) and are linked to the uplift of the East African dome and the establishment of the East African Rift Valley, both of which led to the progressive fragmentation of forested environments in Africa (Pickford 1990; Portik & Blackburn 2016). Thus, the occurrence of a species of *Leptopelis* in the Early Miocene could provide information about an early divergence within *Leptopelis*. In our study, we compared OCO-KOR 502'05d to members of two proposed subgenera, "*Taphriomantis"* and "*Elaphromantis"*, but not "*Heteropelis"* because none of its species were available. The morphology of OCO-KOR 502'05d is almost identical to that of *L. bocagii* (proposed type-species of "*Taphriomantis"* according to Laurent 1941) and *L. nordequatorialis* (closely related to *L. bocagii* according to Portik & Blackburn 2016). Thus, OCO-KOR 502'05d could represent the earliest occurrence of this subgenus of *Leptopelis*.

Divergence between *"Taphriomantis"* and *"Elaphromantis"* (latter represented by *L. notatus* in our study and proposed type-species of "*Elaphromantis"* according to Laurent 1941) was previously estimated to have occurred in the Late Miocene (~10.3 Ma; Portik & Blackburn 2016), but the Early Miocene *Leptopelis* from Chamtwara would push back this divergence by almost 10 million years. We caution that because our study only includes six species of *Leptopelis* and did not sample either the subgenus "*Heteropelis"* or the Ethiopian and Albertine Rift populations of *Leptopelis*, it is possible that the humeral morphology seen in OCO-KOR 502'05d is plesiomorphic for *Leptopelis* rather than for the *"Taphrinomantis"* subgenus, which means OCO-KOR 502'05d may not provide a divergence date between *"Taphrynomantis*" and *"Elaphromantis*".

Palaecology

The generalised morphology of the humerus of the *Leptopelis* from Chamtwara does not offer information on its palaeoecology. The ecologies of extant *Leptopelis* species our fossil species seems to be closely related to (based on humeral resemblance) could provide insight into the palaeoecology of the Early Miocene species. Extant species of *Leptopelis* are mainly arboreal, but several species are known to be terrestrial or fossorial (Portik 2015; Portik & Blackburn 2016). Based on our limited taxonomic sampling, the *Leptopelis* species from Chamtwara is likely closely related to two extant species, the fossorial *L. bocagii* and the arboreal *L. nordequatorialis* (lifestyles according to Portik & Blackburn 2016). Ancestral character reconstruction proposed arboreality to be the ancestral ecology for *Leptopelis*, with fossoriality only evolving once in *L. bocagii* (Portik & Blackburn 2016). If arboreality is ancestral, that implies our extinct *Leptopelis* was an arboreal frog. However, the ecology of *L. nordequatorialis*

has also been reported as terrestrial, not arboreal (Arroyo-Lambaer 2015). If *L. nordequatorialis* is a more terrestrial frog, that raises the possibility that the *Leptopelis* from Chamtwara could have been terrestrial. Until more complete specimens of *Leptopelis* are identified from Chamtwara, we cannot say anything definitive about its palaeoecology.

Palaeoenvironment

Since its initial description in the 1980s, the palaeoenvironment of Chamtwara has been reconstructed, based on its gastropod assemblage, as a humid, tropical rainforest (Pickford 1981, 1983, 2007). Even though modern tropical rainforests host a large diversity of anurans in Africa, Asia and South America (Frost et al. 2006; Feng et al. 2017), almost no fossil anurans have been identified from this environment (for exceptions see: Poinar et al. 1987; Xing et al. 2018; Barcelos & dos Santos 2023). Extant *Leptopelis* species inhabit various environments, from dry grassland to wet rainforest (Schiøtz 1975, 1999). The humerus from Chamtwara resembles two *Leptopelis* species, *L. bocagii* and *L. nordequatorialis*, that both occur in grasslands, rather than tropical forests or rainforests (Channing & Rödel 2019). However, species closely related to *L. nordequatorialis* (and not included in this study; e.g., *L. anchietae*) are known to inhabit wet forested environments (Schiøtz 1975, 1999). Given the diversity of habitats for extant species of *Leptopelis*, it is not possible to use the presence of a *Leptopelis* in Chamtwara to infer or support any specific palaeoenvironment.

Preliminary analyses of Lower Miocene floras in western Kenya reconstructed the palaeoenvironment of Chamtwara and nearby localities as being a tropical forest, but with greater seasonality (Munyaka et al. 2023; Peppe et al. 2023). Recent analyses of the palaeoflora

of the slightly younger and nearby Hiwegi Formation (Rusinga Island, Lake Victoria, Kenya: Fig. 1b) have proposed a greater ranger of palaeohabitats, with a mix of tropical seasonal forest/rainforest and woodland savannah (Maxbauer et al. 2013; Baumgartner & Peppe 2021; Reichgelt & West 2025). Conversely, earlier reconstructions for the Hiweigi Formation based on its gastropod assemblage instead suggested a dry forest (Pickford 1983). It is possible that the palaeoenvironment of Chamtwara was a tropical seasonal forest/rainforest, a woodland savannah, or a transitional environment between the two. It is also possible, as in the Hiwegi Formation, that Chamtwara is composed of a succession of distinct palaeoenvironments over a 1.5 million years span, which cannot be distinguished based on the recovered fauna.

Conclusion

The seven fossil bones reported herein from the rich Lower Miocene fossil locality of Chamtwara, Kenya, pertain to the following anuran taxa: one or more indeterminate anurans; an indeterminate neobatrachian; and an unidentified species of *Leptopelis*. The last is: 1) the first fossil record for the genus *Leptopelis*; 2) the first fossil record for Arthroleptidae; and 3) the oldest reported occurrence for Afrobatrachia, for which the previously known fossil record was limited to the Plio-Pleistocene. The Chamtwara *Leptopelis* species also shares an overall resemblance to both extant *L. bocagii* and *L. nordequatorialis* and could point to the start of the divergence between the *"Taphrinomantis"* and *"Elaphromantis"* subgenera within *Leptopelis*, making it the first marker of diversification within the genus during the Neogene.

Acknowledgements The authors thank Márton Venczel for his works and research on anurans from the Cretaceous of Europe, and his contribution to the knowledge of neobatrachian early evolution and palaeobiogeography. We are grateful to have our paper included in this special issue in his honour. We are also grateful to J. Gardner (Royal Tyrrell Museum of Palaeontology) for his editorial comments on this manuscript. We thank the Department of Herpetology, California Academy of Sciences, the University of Florida, Florida Museum of Natural History Herpetology, The Harvard-Museum of Comparative Zoology the Museum für Naturkunde (Berlin), the Natural History Museum (London) and the University of Texas Biodiversity Center for access to the CT-scans of their specimens for this study. We are grateful to M. Delfino, D. Blackburn, M. Vallejo-Pareja, and T. Matthews for reviewing and commenting on this manuscript.

Funding A. Lemierre was supported by a Dr. Betsy Nicholls Postdoctoral Research Fellowship, provided by the Royal Tyrrell Museum Cooperating Society. Project Paléontologie de l'Afrique Sub-Saharienne (PASS) received funding from the Pôle Sciences humaines et sociales, Archéologie et Patrimoine of the sous-direction de l'Enseignement supérieur et de la Recherche, French Ministry of Europe and Foreign Affairs.

Data availability, A list of 3D models and CT-scan dataset used and produced in this study is available in the Supplementary Data. All 3D models produced for this study are available on MorphoSource: https://www.morphosource.org/projects/000714595

References

Andrews, P., Meyer, G. E., Pilbeam, D. R., Van Couvering, J. A., & Van Couvering, J. A. H. (1981). The Miocene fossil beds of Maboko Island, Kenya: Geology, age, taphonomy and palaeontology. *Journal of Human Evolution*, *10*(1), 35–48. https://doi.org/10.1016/S0047-2484(81)80024-3

Arroyo-Lambaer, D. (2015) *Conserving amphibian diversity: a species inventory and gene flow studies in fragmented montane forest, Mambilla Plateau, Nigeria*. Unpublished PhD thesis University of Canterbury, School of Biological Sciences, Christchurch, New Zealand.

Barcelos, L. A., & dos Santos, R. O. (2023). The Lissamphibian fossil record of South America. *Palaeobiodiversity and Palaeoenvironments*, *103*, 341–405. https://doi.org/10.1007/s12549-022-00536-0

Baumgartner, A., & Peppe, D. J. (2021). Paleoenvironmental changes in the Hiwegi Formation (lower Miocene) of Rusinga Island, Lake Victoria, Kenya. *Palaeobiogeography, Palaeoclimatology, Palaeoecology*, *574*, 110458. https://doi.org/10.1016/j.palaeo.2021.110458

Begun, D. R. (2015). Fossil record of Miocene Hominoids. In W. Henke & I. Tattersall (Eds.), *Handbook of Paleoanthropology* (pp. 1261–1332). Heidelberg: Springer Berlin. https://doi.org/10.1007/978-3-642-39979-4_32

Blackburn, D. C., Boyer D.M., Gray, J. A., Winchester, J., Bates, J. M., Baumgart, S. L., Braker, E., Coldren, D., Conway, K. W., Davis Rabosky, A., de la Sancha, N., Dillman, C. B., Dunnum, J. L., Early, C. M., Frable, B. W., Gage, M. W., Hanken, J., Maisano, J. A., Marks, B. D., Maslenikov, K. P., McCormack, J. E., Nagesan, R. S., Pandelis, G. G., Prestridge, H. L., Rabosky, D. L., Randall, Z. S., Robbins, M. B., Scheinberg, L. A., Spencer, C. L., Summers, A. P., Tapanila, L., Thompson, C. W., Tornabene, L., Watkins-Colwell, G. J., Welton, L. J., the oVert Project Team, & Stanley, E. L. (2024). Increasing the impact of vertebrate scientific collections through 3D-imaging: the openVertebrate (oVert) Thematic Collections Network. *BioScience*, *74*, 169–186.

Blackburn, D. C., Paluh, D. J., Krone, I., Roberts, E. M., Stanley, E. L., & Stevens, N. J. (2019). The earliest fossil of the African clawed frog (genus *Xenopus*) from Sub-Saharan Africa. *Journal of Herpetology*, *53*(2), 125–130. https://doi.org/10.1670/18-139

Blackburn, D. C., Roberts, E. M., & Stevens, N. J. (2015). The earliest record of the endemic African frog family Ptychadenidae from the Oligocene Nsungwe Formation of Tanzania. *Journal of Vertebrate Paleontology*, *35*(2), e907174. https://doi.org/10.1080/02724634.2014.907174

Bolkay, S. J. (1919). Osnove uporedne osteologije anurskih batrahija sa dodatkom o porijeklu Anura i sa skicom naravnoga sistema istih. *Glasnik Zemaljskog Muzeja Bosni Hercegovini*, *31*(4), 277–353.

Channing, A., & Rödel, M.-O. (2019). *Field guide to the frogs & other amphibians of Africa*. Cape Town: Penguin Random House South Africa.

Delfino, M. (2020). Early Pliocene anuran fossils from Kanapoi, Kenya, and the first fossil record for the African burrowing frog *Hemisus* (Neobatrachia: Hemisotidae). *Journal of Human Evolution*, *140*, 102353.

Dodson, P. (1973). The significance of small bones in paleoecological interpretation. *University of Wyoming Contributions to Geology*, *12*(1), 15–19.

Drewes, R. C. (1984) A phylogenetic analysis of the Hyperoliidae (Anura): Treefrogs of Africa, Madagascar, and the Seychelles Islands. *Occasional Papers of the California Academy of Sciences*, *139*, 1–70.

Duméril, C. (1805). *Zoologie analytique, ou méthode naturelle de classification des animaux, rendue plus facile à l'aide de tableaux synoptiques*. Paris: Allais.

Feakins, S. J., & Demenocal, P. B. (2010). Global and African regional climate during the Cenozoic. In L. Werdelin, & W. J. Sanders (Eds.), *Cenozoic mammals of Africa* (pp. 44–56). Berkley: University of California Press.

Fedorov, A., Beichel, R., Kalpathy-Cramer, J., Finet, J., Fillion-Robin, J-C., Pujol, S., Bauer, C., Jennings, D., Fennessy, F. M., Sonka, M., Buatti, J., Aylward, S. R., Miller, J. V., Pieper, S., & Kikinis, R. (2012). 3D Slicer as an image computing platform for the Quantitative Imaging Network. *Magnetic Resonance Imaging*, *30*(9), 1323–1341.

Feng, Y.-J., Blackburn, D. C., Liang, D., Hillis, D. M., Wake, D. B., Cannatella, D. C., & Zhang, P. (2017). Phylogenomics reveals rapid, simultaneous diversification of three major clades of Gondwanan frogs at the Cretaceous–Paleogene boundary. *Proceedings of the National Academy of Sciences*, *114*(29), E5864–E5870. https://doi.org/10.1073/pnas.1704632114

Frost, D. R. (2024). Amphibian species of the world: an online reference. Version 6.2 (24/02/2025). Retrieved [February 25th, 2025] from https://amphibiansoftheworld.amnh.org/index.php. doi.org/10.5531/db.vz.0001

Frost, D. R., Grant, T., Faivovich, J., Bain, R. H., Haas, A., Haddad, C. F. B., De Sá, R. H., Channing, A., Wilkinson, M., Donnellan, S. C., Raxworthy, C. J., Campbell, J. A., Blotto, B. L., Moler, P., Drewes, R. C., Nussbaum, R. A., Lynch, J. P., Green, D. M., Wheeler, W. C. (2006). The Amphibian Tree of Life. *Bulletin of the American Museum of Natural History*, *297*, 1–291. https://doi.org/10.1206/0003-0090(2006)297[0001:TATOL]2.0.CO;2

Gardner, J. D., & Rage, J.-C. (2016). The fossil record of lissamphibians from Africa, Madagascar, and the Arabian Plate. *Palaeobiodiversity and Palaeoenvironments*, *96*(1), 169–220. https://doi.org/10.1007/s12549-015-0221-0

Gómez, R. O. (2016). A new pipid frog from the Upper Cretaceous of Patagonia and early evolution of crown-group Pipidae. *Cretaceous Research*, *62*: 52–64. https://doi.org/10.1016/j.cretres.2016.02.006

Gray, E. (1825). A synopsis of the genera of reptiles and Amphibia, with a description of some new species. *Annals of Philosophy, London*, *10*, 193–217.

Günther, A. C. L. G. (1859*) Catalogue of the Batrachia Salientia in the collection of the British Museum*. London: Taylor and Francis.

Hime, P. M., Lemmon, A. R., Lemmon, E. C. M., Prendini, E., Brown, J. M., Thomson, R. C., Kratovil, J. D., Noonan, B. P., Pyron, R. A., Peloso, P. L. V., Kortyna, M. L., Keogh, J. S., Donnellan, S. C., Lockridge Muller, R., Raxworthy, C. S., Kunte, K., Ron, S. R., Das, S., Gaitonde, N., Green, D. M., Labisko, J., Che, J., Weisrock, D. W. (2021). Phylogenomics reveals ancient gene tree discordance in the amphibian tree of life. *Systematic Biology*, *70*(1), 49–66. https://doi.org/10.1093/sysbio/syaa034

Idris, O. N. (2004). *Taxonomy, phylogeny, and biogeography of the African treefrog species of the genus* Leptopelis *(Hyperoliidae)*. Unpublished PhD thesis, University of Texas, Arlington, Texas, U.S.A.

Jacobs, B. F., Pan, A. D., & Scotese, C. R. (2010). A review of the Cenozoic vegetation history of Africa. In L. Werdelin & W. J. Sanders (Eds.), *Cenozoic mammals of Africa* (pp. 57–72). Berkley: University of California Press.

Laurent, R. F. (1941). Contribution à l'ostéologie et à la systématique des rhacophorides africains. *Revue de Zoologie et de Botanique Africaines, Tervuren*, *35*, 85–111.

Laurent, R. F. (1972). Review: "The morphology, systematics, and evolution of the Old World treefrogs (Rhacophoridae and Hyperoliidae)", by S. S. Liem (1970). *Copeia*, *1972*, 198–201.

Lemierre, A., Vilakazi, N., Gommery, D., & Kgasi, L. (2024). Unveiling the first neobatrachian (Anura) discovered in the paleokarst system of Bolt's Farm (Plio-Pleistocene; Cradle of Humankind), South Africa. *African Journal of Herpetology*, *73*(2), 1–19. https://doi.org/10.1080/21564574.2024.2351821

Matthews, T., & Steininger, C. (2023). A new anuran genus from the fossil sites of Langebaanweg and Cooper's Cave, South Africa. *African Journal of Herpetology*, *72*(2), 1–27. https://doi.org/10.1080/21564574.2023.2251502

Matthews, T., van Dijk, E., Roberts, D. L., & Smith, R. M. H. (2015). An early Pliocene (5.1 Ma) fossil frog community from Langebaanweg, south-western Cape, South Africa. *African Journal of Herpetology*, *64*(1), 39–53. https://doi.org/10.1080/21564574.2014.985261

Maxbauer, D. P., Peppe, D. J., Bamford, M., McNulty, K. P., Harcourt-Smith, W. E. H., & Davis L. E. (2013). A morphotype catalog and paleoenvironmental interpretations of early Miocene fossil leaves from the Hiwegi Formation, Rusinga Island, Lake Victoria, Kenya. *Palaeontologia Electronica*, *16*.3.28A. https://doi.org/10.26879/342

Mivart, S. G. (1869). On the classification of the anurous batrachians. *Proceedings of the Zoological Society of London*, *1869*, 280–295.

Munyaka, V., Oginga, VK. O., Cote, S., Head, J., Lukens, W., Lutz, J. A., Kinyanjui, R. N., Manthi, F. K., Mcnulty, K. P., Hall, A., Tegart, A., Peppe, D. (2023). Reconstructing the climate and ecology of an Early Miocene tropical forest on the flanks of the Tinderet Volcano, Kisumu County, western Kenya. In *Geological Society of America Abstract with Programs* (p. 121-2). 15–18 October, Pittsburgh, Pennsylvania, USA. http://dx.doi.org/10.1130/abs/2023AM-392325

Nečas, T., Badjedjea. G., Volpálenský, M., & Gvoždík, V. (2021). *Congolius*, a new genus of African reed frog endemic to the central Congo: A potential case of convergent evolution. *Scientific Reports*, *11*, 8338. https://doi.org/10.1038/s41598-021-87495-2.

Partridge, T. C. (2010) Tectonics and geomorphology of Africa during the Phanerozoic. In L. Werdelin, & W. J. Sanders (Eds.), *Cenozoic Mammals of Africa* (pp. 3–18). Berkley: University of California Press.

Peppe, D., Mcnulty, K., Cote, S., Head, J., Munyaka, V., Oginga, K. O., Kinyanjui, R. N., Lukens, W. E., Lutz, J. A., Tegart, A. (2023). Paleoclimate reconstructions of the Early Miocene hominoid fossil sites from Chamtwara, Legetet and Koru, Tinderet, western Kenya. *Geological Society of America Abstract with Programs* (p. 121-3). 15–18 October, Pittsburgh, Pennsylvania, USA. https://doi.org/10.1130/abs/2023AM-394907

Pickford, M. (1981). Preliminary Miocene mammalian biostratigraphy for Western Kenya. *Journal of Human Evolution*, *10*(1), 73–97. https://doi.org/10.1016/S0047-2484(81)80026-7

Pickford, M. (1983). Sequence and Environments of the Lower and Middle Miocene Hominoids of Western Kenya. In R. L. Ciochon & R. S. Corruccini (Eds.), *New interpretations of ape and human ancestry* (pp. 421–439). New York and London: Plenum Press.

Pickford, M. (1986). Cainozoic Paleontological sites of Western Kenya. *Münchner Geowissenschaftliche Abhandlungen*, *8*, 1–151.

Pickford, M. (1990). Uplift of the Roof of Africa and its bearing on the evolution of mankind. *Human Evolution, 5*, 1–20.

Pickford, M. (2004). Palaeoenvironments of Early Miocene hominoid-bearing deposits at Napak, Uganda, based on terrestrial molluscs. *Annales de Paléontologie*, *90*(1), 1–12. https://doi.org/10.1016/j.annpal.2003.10.002

Pickford, M. (2007). A new suiform (Artiodactyla, Mammalia) from the Early Miocene of East Africa. *Comptes Rendus Palevol*, *6*(3), 221–229. https://doi.org/10.1016/j.crpv.2006.11.002

Pickford, M., & Kunimatsu, Y. (2005). Catarrhines from the Middle Miocene (ca. 14.5 Ma) of Kipsaraman, Tugen Hills, Kenya. *Anthropological Science*, *113*(2), 189–224. https://doi.org/10.1537/ase.113.189

Poinar, Jr., G. O., & Cannatella, D. C. (1987). An Upper Eocene frog from the Dominican Republic and its implications for Caribbean biogeography. *Science*, *237*, 1215–1216.

Portik, D. (2015). *Diversification of afrobatrachian frogs and the herpetofauna of the Arabian Peninsula*. Unpublished PhD thesis, University of California, Berkeley, California, USA.

Portik, D., & Blackburn, D. C. (2016). The evolution of reproductive diversity in Afrobatrachia: A phylogenetic comparative analysis of an extensive radiation of African frogs. *Evolution*, *70*(9), 2017–2032.

Portik, D., Striecher, J. W., & Wiens, J. J. (2023). Frog phylogeny: A time-based calibrated, species-level tree based on hundreds of loci and 5,242 species. *Molecular Phylogenetics and Evolution*, *188*, 107907.

Portillo, F., Greenhaum, E., Menegon, M., Kusamba, C., & Dehling, M. J. (2015). Phylogeography and species boundaries of *Leptopelis* (Anura: Arthroleptidae) from the Albertine Rift. *Molecular Phylogenetics and Evolution*, *82*(Part A), 75–86.

Rage, J.-C., & Pickford, M. (2011). Discovery of a gymnophionan skull (?Caeciliidae, Amphibia) in the Early Miocene of Uganda. *Geo-Pal Uganda*, *4*, 1–9.

Reichgelt T., & West C. K. (2025). Insights into greener Miocene biomes and globally enhanced terrestrial productivity from fossil leaves. *Evolving Earth*, *3*, 100058. https://doi.org/10.1016/j.eve.2025.100058

Reig, O. (1958). Proposiciones para una nueva macrosistemática de los anuros (nota preliminar). *Physis*, *21*(60), 109–118.

Reyes-Velasco, J., Manthey, J. D., Freilich, X., & Boissinot, S. (2018). Diversification of African tree frogs (genus *Leptopelis*) in the highlands of Ethiopia. *Molecular Ecology*, *27*, 2256–2270. https://doi.org/10.1111/mec.14573

Sanchíz, B. (1998). *Salientia*. In P. Wellnhofer (Ed.) *Handbuch der Paläoherpetologie*, *Part 4* (pp. 1–276). Stuttgart: Gustav Fischer Verlag.

Schiøtz, A. (1975). *The treefrogs of eastern Africa*. Copenhagen: Seenstrupia.

Schiøtz, A. (1999). *Treefrogs of Africa*. Frankfurt am Maine: Edition Chimaira.

Scott, E. (2005) A phylogeny of ranid frogs (Anura: Ranoidea: Ranidae), based on a simultaneous analysis of morphological and molecular data. *Cladistics*, *21*(6), 507–574. https://doi.org/10.1111/j.1096-0031.2005.00079.x

Spawls, S., Wasonga, D. V., & Drewes, R. C. (2019). *The amphibians of Kenya*. Stephen Spawls (privately published).

Tappen, M. (1994). Bone weathering in the tropical rain forest. *Journal of Archaeological Science*, *21*(5), 667–673.

Van Dijk, D. E. (2001). Osteology of the ranoid burrowing African anurans *Breviceps* and *Hemisus*. *African Zoology*, *36*(2), 137–141.

Xing, L., Stanley, E. L., Bai, M., & Blackburn, D. C. (2018). The earliest direct evidence of frogs in wet tropical forests from Cretaceous Burmese amber. *Scientific Reports, 8*(1). https://doi.org/10.1038/s41598-018-26848-w

Figure Captions

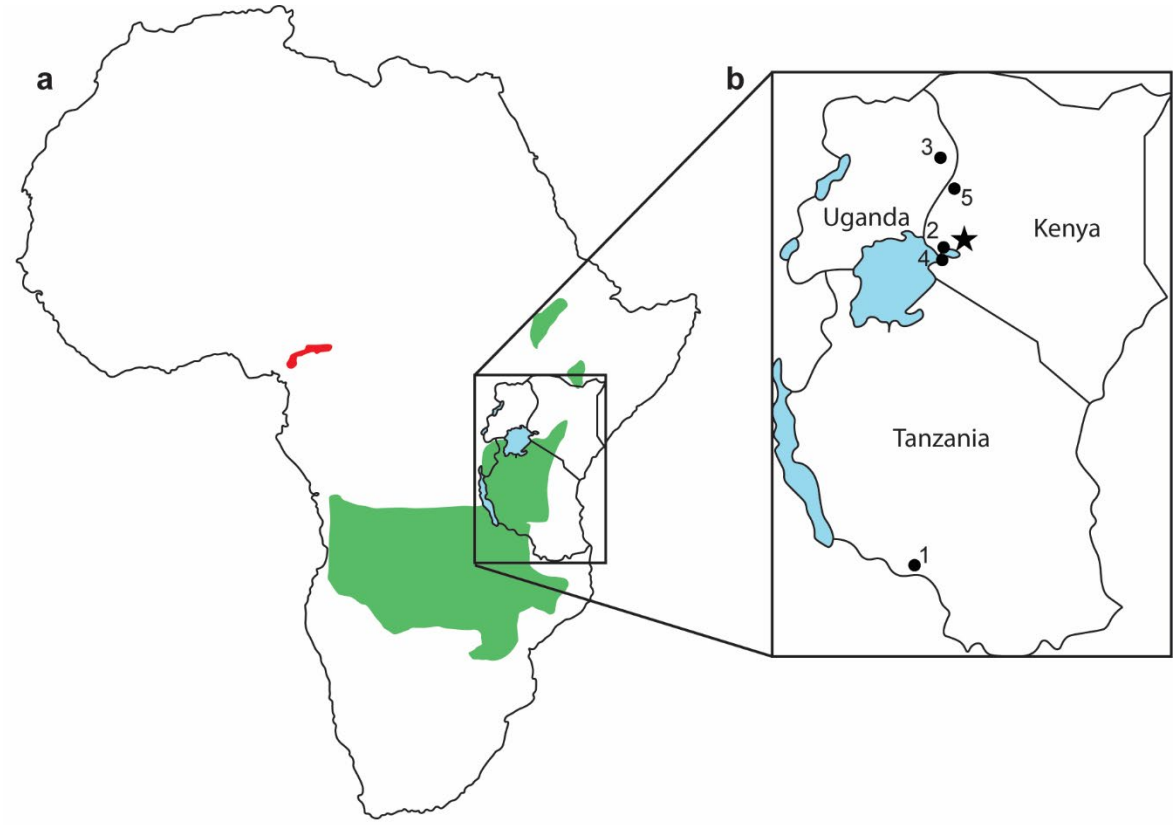
a
b
Uganda
Kenya
Tanzania
1
2
3
4
5


c

Fig. 1. Map and photograph of the Chamtwara locality. **a, b**, Maps showing the location of Chamtwara (star), other mentioned localities in East Africa and areas where *Leptopelis bocagii* (green) and *L. nordequatorialis* (red) are found; **c**, photograph of the locality. Localities are as follows: *1*, Nsungwe Formation, Tanzania; *2*, Maboko Island, Kenya; *3*, Napak XV, Uganda; *4*, Rusinga Island, Kenya; and *5*, Kanapoi, Kenya. [full page width]

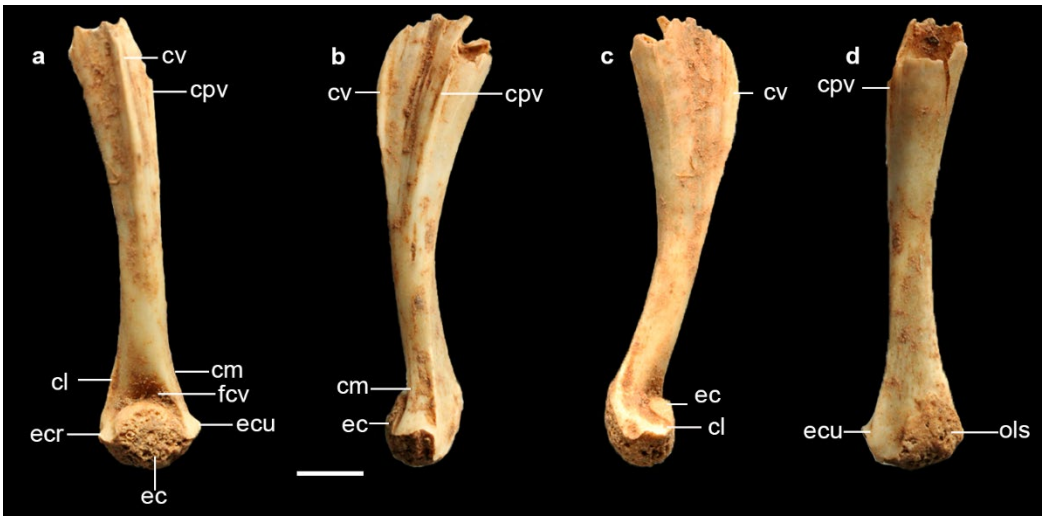

Fig. 2. Photographs of right humerus of *Leptopelis* sp. (OCO-KOR 502'05d) from the Lower Miocene of Chamtwara in ventral (**a**), medial (**b**), lateral (**c**) and dorsal (**d**) views. Abbreviations: *cl* crista lateralis; *cm* crista medialis; *cpv* crista paraventralis; *cv* crista ventralis; *ec* eminentia capitata; *ecr* epicondylus radialis; *ecu* epicondylus ulnaris; *fcv* fossa cubitalis ventralis; *ols* olecranon scar. Scale bar equals 2 mm. [full page width]

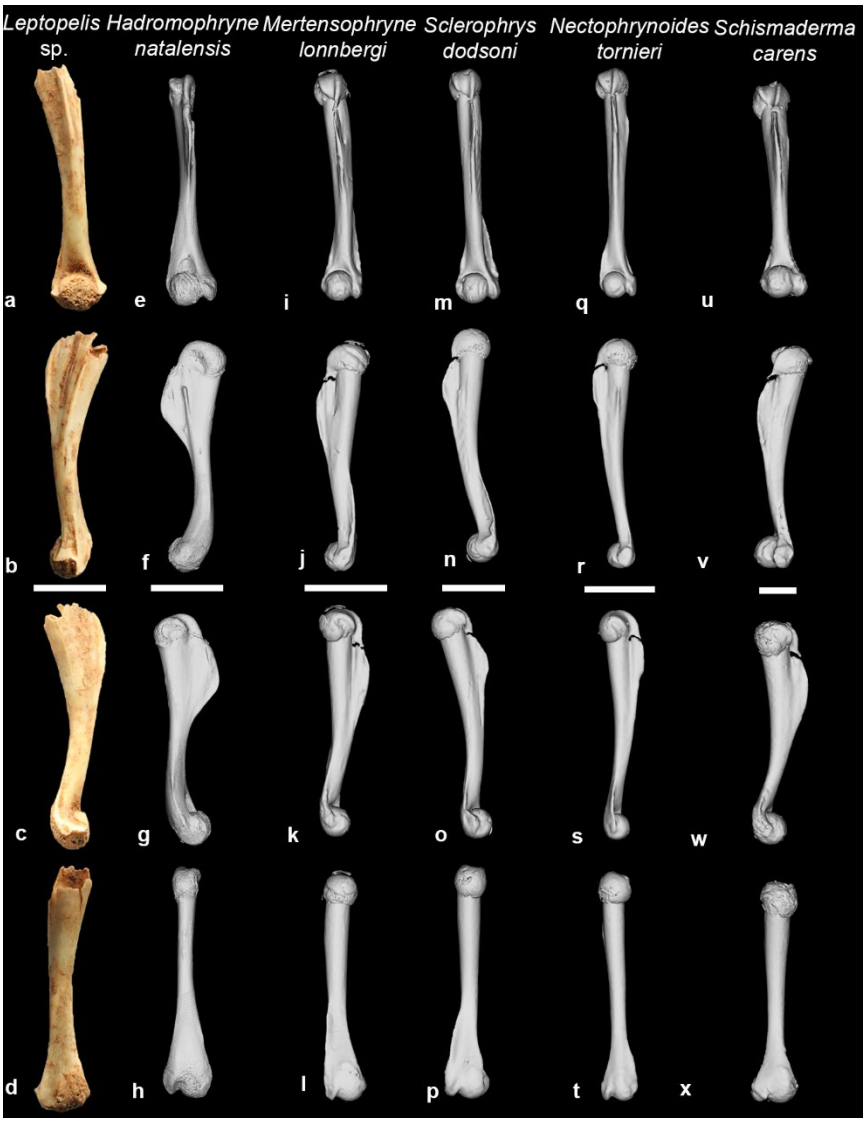

Fig. 3. Right humeri of *Leptopelis* sp. from the Lower Miocene of Chamtwara and representatives of extant species of Heleophrynidae and Bufonidae genera from Sub-Saharan Africa. **a**–**d**, *Leptopelis* sp. (OCO-KOR 502'05d) in ventral (**a**), medial (**b**), lateral (**c**) and dorsal (**d**) views; **e**–**h**, *Hadromophryne natalensis* (Heleophrynidae, UF-HERP: 100828) in ventral (**e**), medial (**f**), lateral (**g**) and dorsal (**h**) views; **i**–**l**, *Mertensophryne lombergi* (Bufonidae, UF-HERP: 92078) in ventral (**i**), medial (**j**), lateral (**k**) and dorsal (**l**) views; **m**–**p**, *Sclerophrys dodsoni* (Bufonidae, CAS:HERP:196558) in ventral (**m**), medial (**n**), lateral (**o**) and dorsal (**p**) views; **q**–**t**, *Nectophrynoides tornieri* (Bufonidae; CAS:HERP:125439) in ventral (**q**), medial (**r**), lateral (**s**)

and dorsal (**t**) views; **u**–**x**, *Schismaderma carens* (Bufonidae, CAS: HERP: 227515) in ventral (**u**), medial (**v**), lateral (**w**) and dorsal (**x**) views; and **y**–**bb**, in ventral (**y**), medial (**z**), lateral (**aa**) and dorsal (**bb**) views. **a**–**d** are photographs of OCO-KOR 502'05d, whereas **e**–**x** are 3D models. Images at different magnifications; see corresponding 4 mm (**a**–**p**; **u**–**x**) and 2.5 mm (**q**–**t**) scale bars. [full page width]

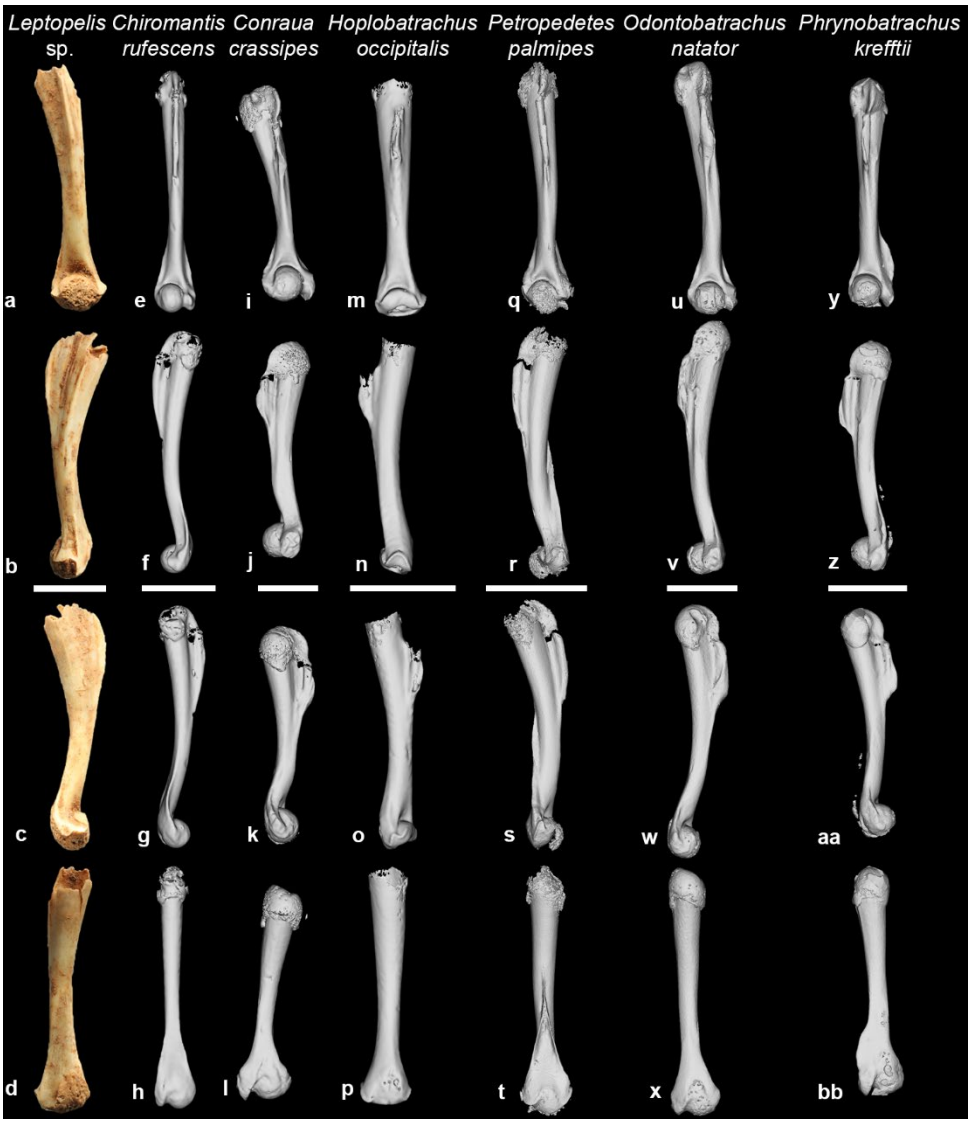

Fig. 4. Right humeri of *Leptopelis* sp. from the Lower Miocene of Chamtwara and representatives of extant species of non-pyxicephalid natatanura genera from Sub-Saharan

Africa. **a**–**d**, *Leptopelis* sp. (OCO-KOR 502'05d) in ventral (**a**), medial (**b**), lateral (**c**) and dorsal (**d**) views; **e**–**h**, *Chiromantis rufescens* (Rhacophoridae, CAS:HERP:253330) in ventral (**e**), medial (**f**), lateral (**g**) and dorsal (**h**) views; **i**–**l**, *Conraua crassipes* (Conrauidae, CAS:HERP:258122) in ventral (**i**), medial (**j**), lateral (**k**) and dorsal (**l**) views; **m**–**p**, *Hoplobatrachus occipitalis* (juvenile, Discroglossidae; CAS:HERP:168679) in ventral (**m**), medial (**n**), lateral (**o**) and dorsal (**p**) views; **q**–**t**, *Petropedetes palmipes* (Petropedetidae, CAS:HERP:153715) in ventral (**q**), medial (**r**), lateral (**s**) and dorsal (**t**) views; **u**–**x**, *Odontobatrachus natator* (Petropedetidae, CAS:HERP:230204) in ventral (**u**), medial (**v**), lateral (**w**) and dorsal (**x**) views; and **y**–**bb**, *Phrynobatrachus krefftii* (Phrynobatrachidae, CAS: HERP: 18618) in ventral (**y**), medial (**z**), lateral (**aa**) and dorsal (**bb**) views. **a**–**d** are photographs of OCO-KOR 502'05d, whereas **e**–**bb** are 3D models. Images at different magnifications; see corresponding 4 mm scale bars. [full page width]

Fig. 5. Right humeri of *Leptopelis* sp. from the Lower Miocene of Chamtwara and representatives of extant species of ptychadenid, ranid and pyxicephalid natatanura genera from Sub-Saharan Africa. **a**–**d**, *Leptopelis* sp. (OCO-KOR 502'05d) in ventral (**a**), medial (**b**), lateral (**c**) and dorsal (**d**) views; **e**–**h**, *Ptychadena oxyrhynchus* (Ptychadenidae, CAS:HERP:256821) in ventral (**e**), medial (**f**), lateral (**g**) and dorsal (**h**) views; **i**–**l**, *Amnirana albolaris* (Ranidae, CAS:HERP:258101) in ventral (**i**), medial (**j**), lateral (**k**) and dorsal (**l**) views; **m**–**p**, *Pyxicephalus adspersus* (Pyxicephalidae, Pyxicephalinae, UF-HERP:92093) in ventral (**m**), medial (**n**), lateral (**o**) and dorsal (**p**) views; **q**–**t**, *Cacosternum boettgeri* (Pyxicephalidae, Cacosterninae,

CAS:HERP:125890) in ventral (**q**), medial (**r**), lateral (**s**) and dorsal (**t**) views; **u**–**x**, *Strongylopus grayii* (Pyxicephalidae, Cacosterninae, CAS:HERP:211614) in ventral (**u**), medial (**v**), lateral (**w**) and dorsal (**x**) views and **y**–**bb**, *Tomopterna delalandii* (Pyxicephalidae, Cacosterninae, CAS:HERP:157511) in ventral (**y**), medial (**z**), lateral (**aa**) and dorsal (**bb**) views. **a**–**d** are photographs of OCO-KOR 502'05d, whereas **e**–**bb** are 3D models. Images at different magnifications; see corresponding 4 mm (**a**–**l**; **q**–**bb**) and 2.5 mm (**m**–**p**) scale bars. [full page width]

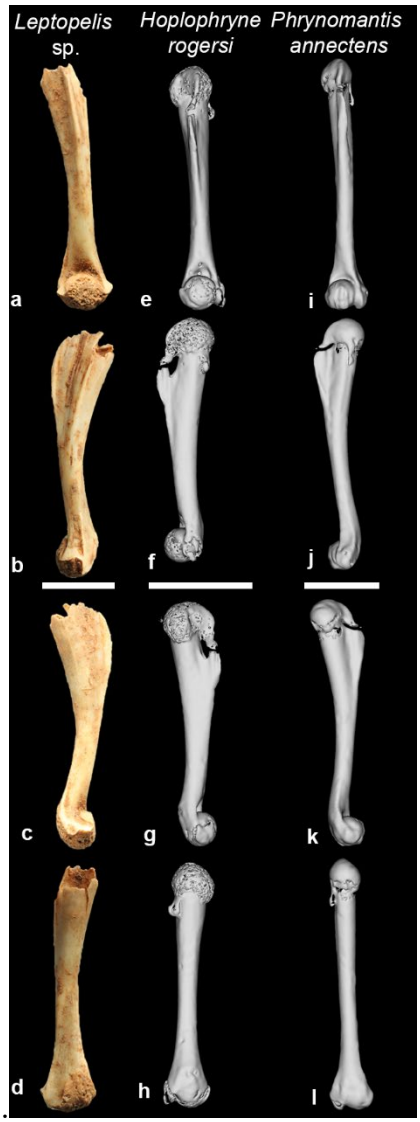

Fig. 6. Right humeri of *Leptopelis* sp. from the Lower Miocene of Chamtwara and representatives of extant species microhylid genera from Sub-Saharan Africa. **a**–**d**, *Leptopelis* sp. (OCO-KOR 502'05d) in ventral (**a**), medial (**b**), lateral (**c**) and dorsal (**d**) views **e**–**h**, *Hoplophryne rogersi* (Hoplophryninae, CAS:HERP:168679) in ventral (**e**), medial (**f**), lateral (**g**) and dorsal (**h**) views and **i**–**l,** *Phrynomantis annectens* (Phrynomerinae, UF-HERP:187273) in ventral (**i**), medial (**j**), lateral (**k**) and dorsal (**l**) views. **a**–**d** are photographs of OCO-KOR

502’05d, whereas **e**–**l** are 3D models. Images at different magnifications; see corresponding 4 mm (**a**–**d**) and 2.5 mm (**e**–**l**) scale bars. [1/3 page width]

Fig. 7. Right humeri of *Leptopelis* sp. from the Lower Miocene of Chamtwara and representatives of extant species of hyperoliid genera from Sub-Saharan Africa. **a**–**d**, *Leptopelis* sp. (OCO-KOR 502’05d) in ventral (**a**), medial (**b**), lateral (**c**) and dorsal (**d**) views; **e**–**h**, *Hyperolius schoutedeni* (Hyperoliidae, Hyperoliinae, UF-HERP:185889) in ventral (**e**), medial

(**f**), lateral (**g**) and dorsal (**h**) views; **i**–**l**, *Ophisthothylax immaculatus* (Hyperoliidae, Hyperoliinae CAS:HERP:258235) in ventral (**i**), medial (**j**), lateral (**k**) and dorsal (**l**) views; **m**–**p**, *Chrysobatrachus cupreonitens* (Hyperoliidae, incertia sedis, UF-HERP:27884) in ventral (**m**), medial (**n**), lateral (**o**) and dorsal (**p**) views; **q**–**t**, *Hylambates leonardi* (Hyperoliidae, Kassinae, CAS:HERP:258273) in ventral (**q**), medial (**r**), lateral (**s**) and dorsal (**t**) views; **u**–**x**, *Kassina senegalensis* (Hyperoliidae, Kassinae, UF-HERP:28288) in ventral (**u**), medial (**v**), lateral (**w**) and dorsal (**x**) views; and **y**–**bb**, *Paracassina kouhiensis* (Hyperoliidae, Kassinae, CAS:HERP:145356) in ventral (**y**), medial (**z**), lateral (**aa**) and dorsal (**bb**) views. **a**–**d** are photographs of OCO-KOR 502'05d, whereas **e**–**bb** are 3D models. Images at different magnifications; see corresponding 4 mm (**a**–**d**; **q**–**bb**) and 2.5 mm (**e**–**p**) scale bars. [full page width]

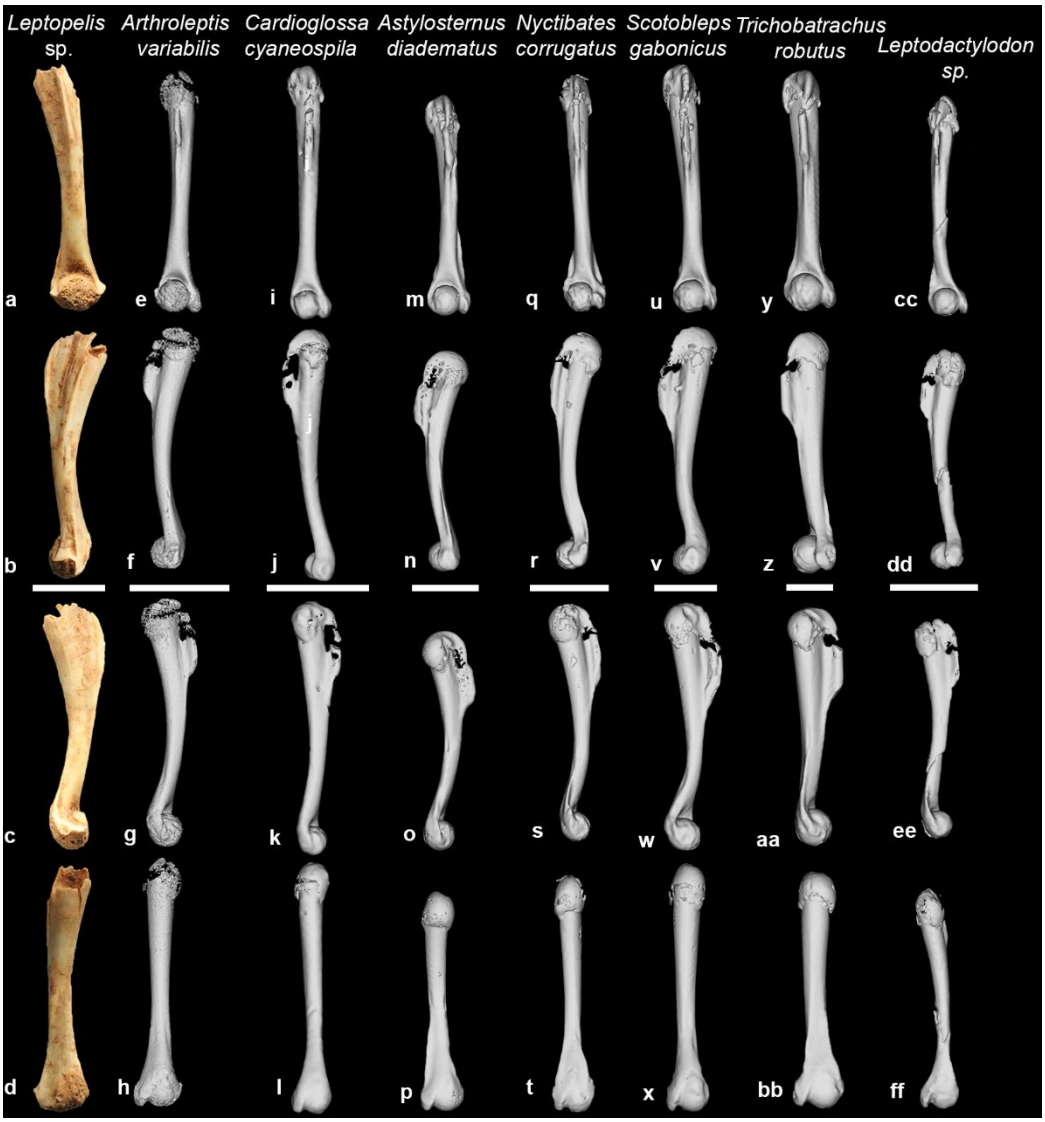

Fig. 8. Right humeri of *Leptopelis* sp. from the Lower Miocene of Chamtwara and representatives of extant species of arthroleptid genera from Sub-Saharan Africa. **a**–**d**, *Leptopelis* sp. (OCO-KOR 502'05d) in ventral (**a**), medial (**b**), lateral (**c**) and dorsal (**d**) views; **e**–**h**, *Arthroleptis variabilis* (Arthroleptidae, Arthroleptinae, ZMB 70086) in ventral (**e**), medial (**f**), lateral (**g**) and dorsal (**h**) views; **i**–**l**, *Cardioglossa cyaneospila* (Arthroleptidae, Arthroleptinae, CAS:HERP:250950) in ventral (**i**), medial (**j**), lateral (**k**) and dorsal (**l**) views; **m**–**p**, *Astylosternus diadematus* (Arthroleptidae, Astylosterninae, CAS:HERP:254126) in ventral (**m**), medial (**n**), lateral (**o**) and dorsal (**p**) views; **q**–**t**, *Nyctibates corrugatus* (Arthroleptidae,

Astylosterninae, UF-HERP:190730) in ventral (**q**), medial (**r**), lateral (**s**) and dorsal (**t**) views; **u**–**x**, *Scotobleps gabonicus* (Arthroleptidae, Astylosterninae, CAS:HERP:25686) in ventral (**u**), medial (**v**), lateral (**w**) and dorsal (**x**) views; **y**–**bb**, *Trichobatrachus robustus* (Arthroleptidae, Astylosterninae, CAS:HERP:254134) in ventral (**y**), medial (**z**), lateral (**aa**) and dorsal (**bb**) views; and **cc**–**ff**, *Leptodactylodon* sp. (Arthroleptidae, Astylosterninae, CAS:HERP:260136) in ventral (**cc**), medial (**dd**), lateral (**ee**) and dorsal (**ff**) views. **a**–**d** are photographs of OCO-KOR 502'05d, whereas **e**–**ff** are 3D models. Images at different magnifications; see corresponding 4 mm (**a**–**bb**) and 2.5 mm (**cc**–**ff**) scale bars. [full page width]

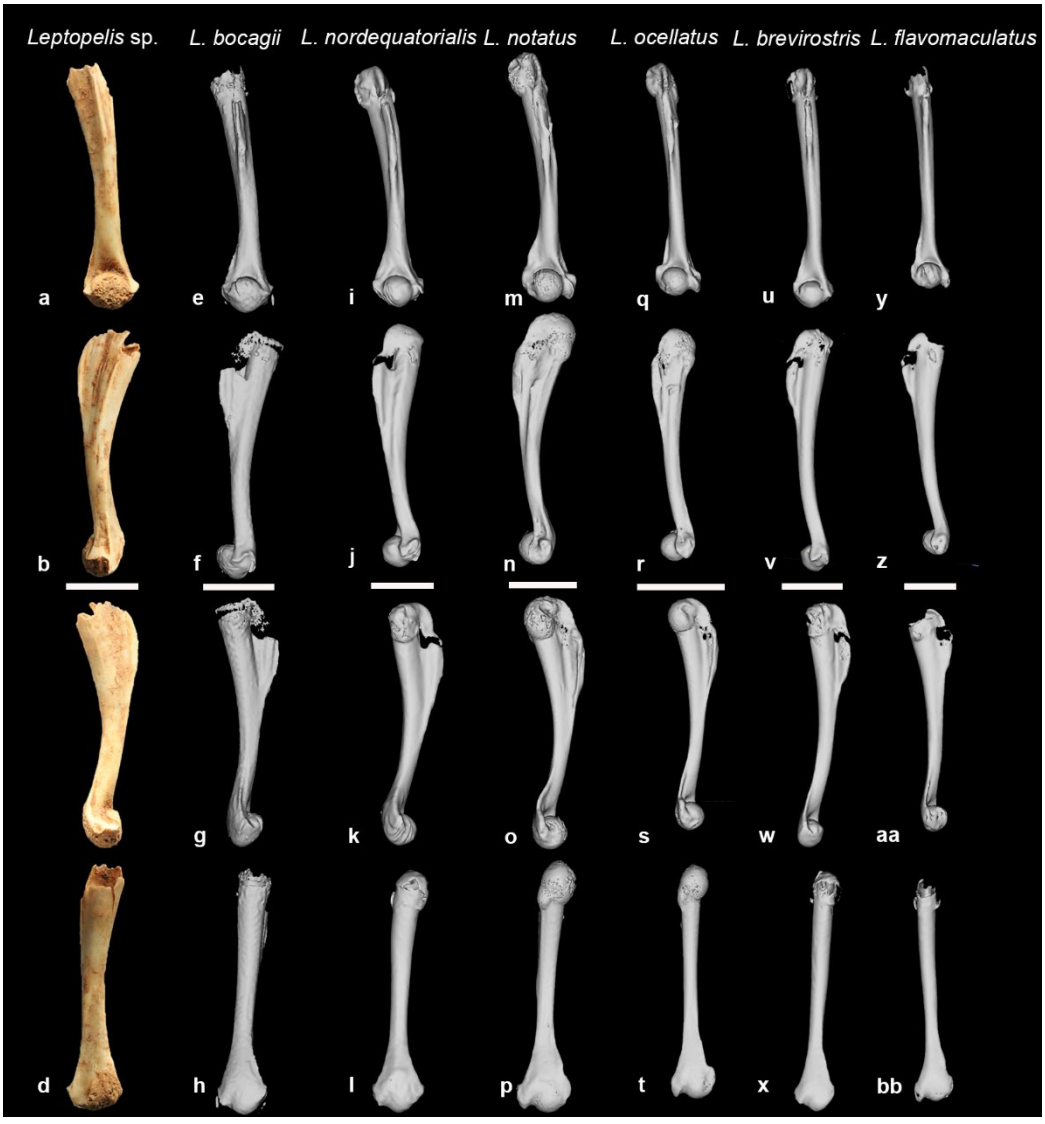

Fig. 9. Right humeri of *Leptopelis* sp. from the Early Miocene of Chamtwara and representatives of extant species of *Leptopelis* from Sub-Saharan Africa. **a**–**d**, *Leptopelis* sp. (OCO-KOR 502'05d) in ventral (**a**), medial (**b**), lateral (**c**) and dorsal (**d**) views; **e**–**h**, *L. bocagii* (CAS: HERP: 1545180) in ventral (**e**), medial (**f**), lateral (**g**) and dorsal (**h**) views; **i**–**l**, *L. nordequatorialis* (CAS: HERP: 253625) in ventral (**i**), medial (**j**), lateral (**k**) and dorsal (**l**) views; **m**–**p**, *L. notatus* (CAS: HERP: 253554) in ventral (**m**), medial (**n**), lateral (**o**) and dorsal (**p**) views; **q**–**t**, *L. ocellatus* (CAS: HERP: 253513) in ventral (**q**), medial (**r**), lateral (**s**) and dorsal (**t**) views; **u**–**x**, *L. brevirostris* (CAS: HERP: 260137) in ventral (**u**), medial (**v**), lateral (**w**) and dorsal (**x**) views; and **y**–**bb**, *L. flavomaculatus* (CAS: HERP: 18618) in ventral (**y**), medial (**z**), lateral (**aa**) and dorsal (**bb**) views. **a**–**d** are photographs of OCO-KOR 502'05d, whereas **e**–**bb** are 3D models. Images at different magnifications; see corresponding 5 mm (**e**–**p**), 4 mm (**a**–**d**), 2.5 mm (**e**–**p**) and 2 mm (**y**–**bb**) scale bars. [full page width]

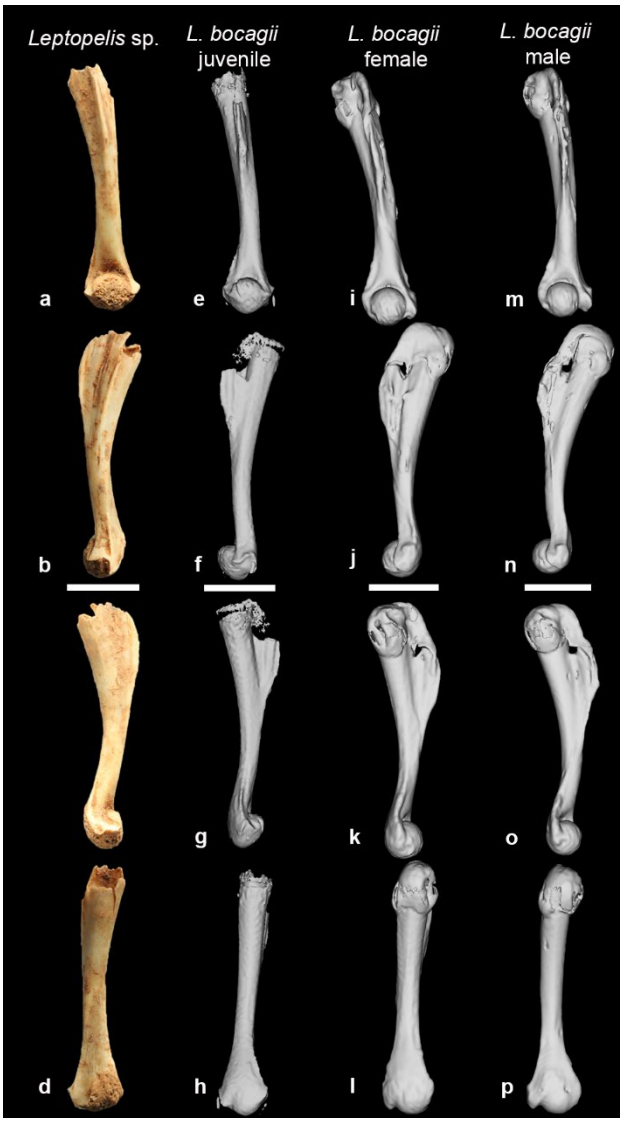

Fig. 10. Right humeri of *Leptopelis* sp. from the Early Miocene of Chamtwara and three individuals of *Leptopelis bocagii*. **a**–**d**, *Leptopelis* sp. (OCO-KOR 502'05d) in ventral (**a**), medial (**b**), lateral (**c**) and dorsal (**d**) views; **e**–**h**, juvenile of *L. bocagii* (CAS: HERP: 1545180) in ventral (**e**), medial (**f**), lateral (**g**) and dorsal (**h**) views; **i**–**l**, female adult of *L. bocagii* (UF-HERP:183604) in ventral (**i**), medial (**j**), lateral (**k**) and dorsal (**l**) views; and **m**–**p**, male adult of *L. bocagii* (UF-HERP:183603) in ventral (**m**), medial (**n**), lateral (**o**) and dorsal (**p**) views. Images at different magnifications; see corresponding 4 mm (**a**–**d**; **i**–**p**) and 2.5 mm (**e**–**h**) scale bars. [1/2 page width]

Fig. 11. Postcranial elements of Neobatrachia indet. and Anura indet. from the Lower Miocene of Chamtwara. **a**–**b**, distal portion of left humerus of Neobatrachia indet. (OCO-KOR 502'05e) in ventral (**a**) and dorsal (**b**) views; **c,** proximal? portion of femur of Anura indet. (OCO-KOR 502'05f) in transverse view; and **d**, fragment of tibiofibula of Anura indet. (side uncertain; OCO-KOR 502'05g) in dorsal or ventral views. Abbreviations: *ec*, eminentia capitata; *ecr*, epicondylus radialis; *ecu* epicondylus ulnaris; *fcv* fossa cubitalis ventralis; *ols* olecranon scar. Images at same magnification, scale bar equals 5 mm. [full page width]